Testing and Analysis of 'Bare' Superconducting Radio-Frequency Cavities

Cole Cook

Department of Physics and Astronomy, University of Wisconsin Eau Claire, Eau Claire, WI 54702-4004

Elvin Harms, Jr.

Accelerator Division, Superconducting Radio-Frequency Beam Test Facility Department, Fermilab, Batavia, IL

Abstract

Superconductivity was discovered 100 years ago. In 100 years, advances have been made but there is still much to learn about superconductivity and the uses of superconductive materials. At Fermilab, research and development is being done in order to understand the properties and uses of various superconducting materials to advance the fields of accelerator and high energy physics though more efficient and higher capacity components. These superconducting materials may be used to make magnets or radio-frequency cavities for future accelerators. In the case of radio-frequency cavities, superconductors are being used in order to minimize the power dissipated and increase the figures of merit of a radio-frequency cavity, such as the quality factor and accelerating gradient. Switching from copper cavities, a non-superconducting metal, to niobium cavities, a superconducting metal, processing techniques must be analyzed in order to maximize these figures of merit. The effects of three processing procedures are currently being studied: baking the cavity at 120°C and cleaning the inner surface by either buffered chemical polishing or electropolishing. Studying these different processing techniques has proved challenging as problems have arisen in the both the cryosystem and power meters. This paper will address these problems and illustrate the importance of well working equipment.

Introduction

Superconducting Radio-Frequency (SRF) cavities are made using high purity niobium. The reason for this is that niobium has the highest critical temperature at which it goes superconducting for a pure metal. Additionally, niobium is easy to machine at room temperature and has been used to make a multitude of other superconducting objects.

SRF cavities are currently being used in some accelerators, such as the Large Hadron Collider (LHC) at CERN, Argonne Tandem Linac Accelerator System (ATLAS) at Argonne National Laboratory, the Continuous Electron Beam Accelerator Facility (CEBAF) at Thomas Jefferson National Accelerator Facility, the Spallation Neutron Source (SNS) at Oak Ridge National Laboratory and the Free-electron LASer in Hamburg (FLASH) at DESY. However, in order to get to higher particle energies or reduce costs for use in LINACs, SRF cavities must have better accelerating gradients and quality factors. In order to make better SRF cavities, fabrication techniques must be analyzed to find the combination of techniques giving the best results in accelerating gradients and quality factors.

Fabricating and processing of a SRF cavity is a multistep process which is outlined in Hasan Padamsee's two books.[2,3] It begins with sheets of niobium that are inspected for numerous factors such as an absence of scratches. Then the sheets are formed into half-cells which will be electron welded together. Before welding, iron is removed using sulfuric acid followed by a water bath for twelve hours and a 20μm etch.

After welding, the cavity is cleaned ultrasonically and baked at 800°C. This baking is done to get rid of the hydrogen gas that may have been trapped in the cavity walls due to exposure to acid. After this, an inner surface treatment will be used to remove particulates and imperfections. In order to remove residue and particulates, a high pressure rinse using high purity water is used.

Two of the processing techniques being analyzed involve inner surface treatment of the SRF cavity. These two techniques are buffered chemical polishing (BCP) and electropolishing (EP). Both of these techniques involve etching the surface with an acid solution. The solution removes particulates and imperfections in the inner surface of a cavity, thus, creating a "smooth" inner surface. There are three differences between BCP and EP. The first is that the acid solution for BCP is one part HF (40%), one part HNO_3 (65%), and two parts H_3PO_4 (85%) by volume whereas the acid solution for EP is one part HF (40%) and nine parts H_2SO_4 (98%) by volume.

The numbers in parentheses is the industrial strength of the acid. The second is the temperature at which the two solutions are used. EP is done at 30°C while BCP is done below 15°C. The final difference is that EP involves inserting an anode in the acid solution, inducing a current that flows through the acid and to the cathode, the cavity.

Another preparation technique being looked at is the effect of baking a cavity at 120°C for 24 to 48 hours. This is thought to allow the quality factor to remain constant with higher accelerating gradient.

While testing cavities to find the maximum accelerating gradient, electrons may be produced. Electrons can be produced in a cavity when unwanted particulates or imperfections inside the cavity become excited by high electric fields and release electrons into the cavity. Since the highest electric fields are at the iris of the cells, this is the most likely location for electron production. These electrons could hit a wall of the cavity and produce x-rays. This will produce a localized heating and potentially quench the cavity.

A quench is a rapid heating of an area of the cavity that can cause the metal to heat past its critical temperature and lose its superconducting properties, such as zero surface resistance. There are two different types of quenches: global or local quenches. A global quench is typically found at the equator of a SRF cavity and is quite fast. This is because this is the location of the largest magnetic field. Superconductors have a maximum magnetic field they can withstand as a function of temperature and still remain superconducting. If the magnetic field is above this maximum, the material is no longer superconducting. This increases the surface resistance and the increased surface resistance will cause a global heating, thus quenching the cavity. Additionally, a global quench can occur due to magnetic heating increasing the surface temperature of the cavity.

A local quench, on the other hand, typically is due to electrons hitting the wall of a cavity. Therefore, a local quench originates at the iris of a cavity. This causes more of a localized heating as the particles could be hitting a localized area of the cavity. Additionally it takes longer than a hard quench as particles must hit the cavity walls repeatedly in order to raise the temperature above the critical temperature.

If a cavity is found to have the acceptable figures of merit, it may be ‘dressed’ for a cryomodule, a string of cavities. These figures of merit include the accelerating gradient and the quality factor. The accelerating gradient is the available number of volts per meter that the

particle is accelerated through which is specified for each accelerator. The quality factor is the ratio of the energy gained to the power dissipated in one rf cycle. For an SRF cavity, the quality factor should be around 10^{10}. The difference between a 'bare' and 'dressed' cavity is that the individual cells can be seen in a 'bare' cavity. A 'dressed' cavity has had a helium vessel and tuner installed. This helium vessel is similar to a thermos; it contains the cavity and a little more than enough liquid helium to keep the cavity superconducting. The tuner allows the resonant frequency of the cavity to be adjusted. This tuner is needed so that the cavities in a cryomodule have the same resonant frequency and to adjust for temperature fluctuations.

Experimental

Setup

A SRF cavity is lowered vertically into a bath of liquid helium (Figure 1&2). This bath is initially around 4K boiling at atmospheric pressure when data is first taken. The testing starts with an RF generator. This generator produces the signal frequency and amplitude, pulse width and repetition rate that will create the electromagnetic fields in the SRF cavity that would accelerate particles in an accelerator. This signal is then split so the phase can be measured with respect to the phase of the forward power. If necessary, the RF signal is phase shifted and amplified. The now shifted and amplified signal is sent through a directional coupler and into the cavity. A directional coupler is used to measure both the forward and reflected powers immediately at the input to the cavity because some of the power at input is reflected back. If one did not use a directional coupler, one could obtain interference between the forward and reflected powers.

Figure 1 – A picture of a cavity before being lowered into the dewar. The plastic rings hold the second sound quench detectors.

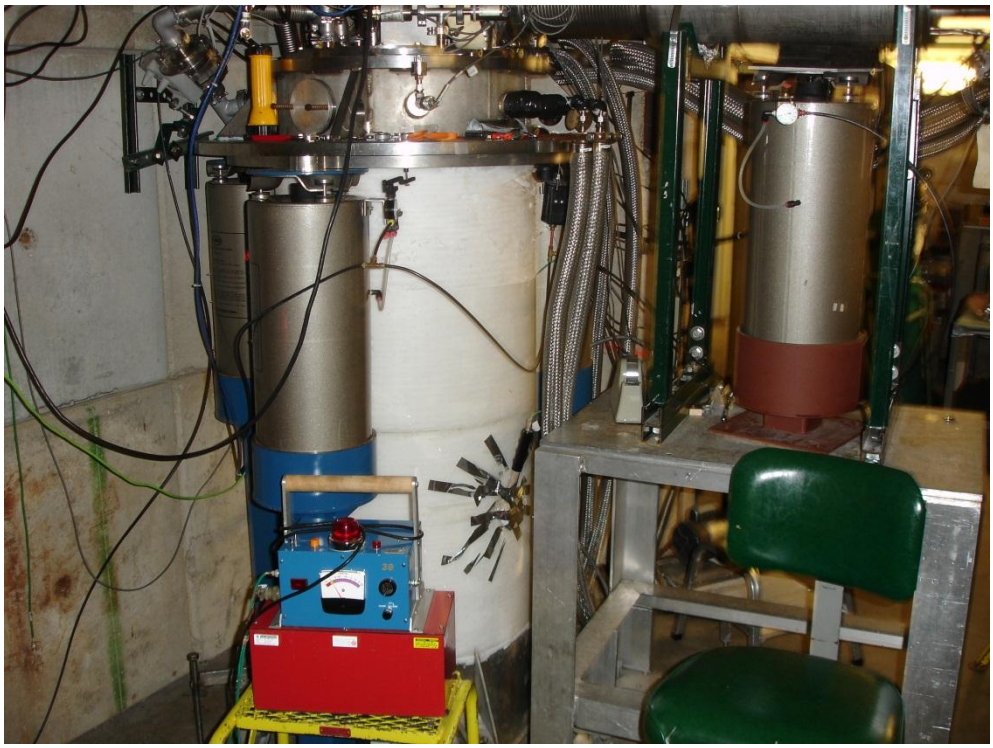

Figure 2 - The large white cylindrical object contains the cavity and the liquid helium required to cool the cavity. The blue box in front is one of the calibrated Geiger counters that can shut down a test in progress.

Some of the power is reflected back at the input coupler while most of the power is transmitted through the cavity to be detected on the other side. Each of the three powers: forward, reflected and transmitted, are then split enabling a scalar measurement to be made using a power meter and waveform analysis to be done using an oscilloscope. The reflected and transmitted powers are looked at using the same oscilloscope while the forward and RF signal are looked both looked at on another (Figure 3&4). For a graphical representation of this setup, see Appendix A.

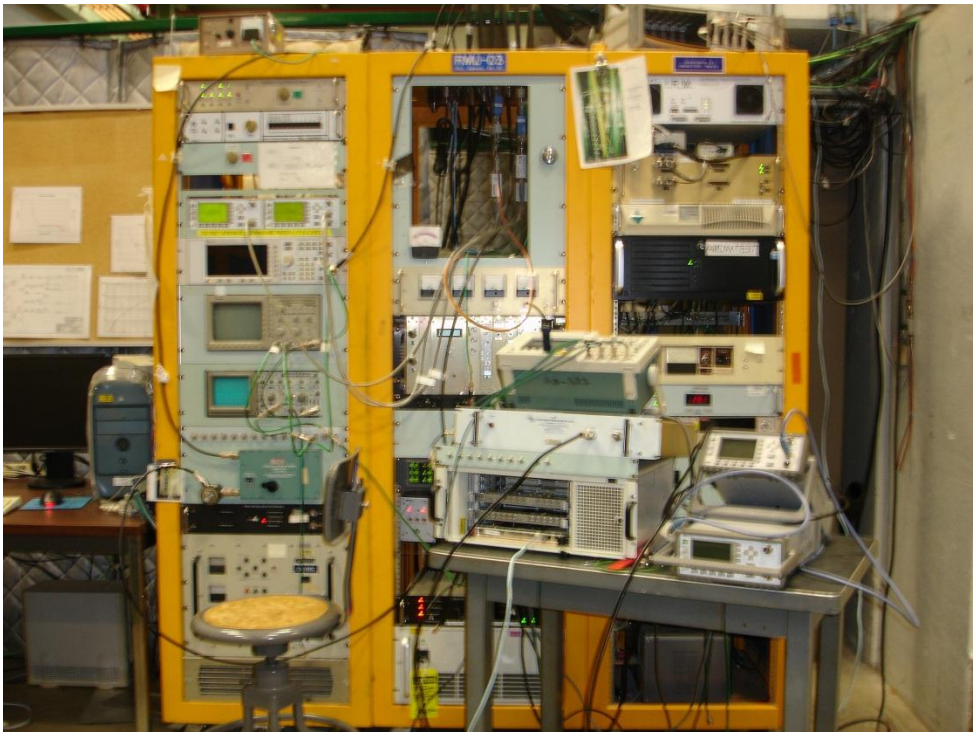

Figure 3 - Image of the racks containing equipment needed to test an SRF cavity. This includes power meters, RF signal generator and oscilloscopes.

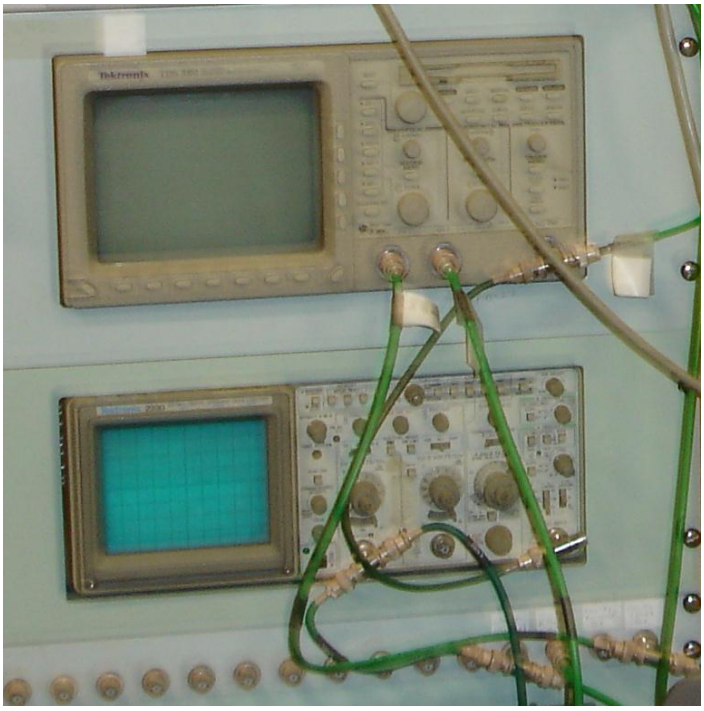

Figure 4 – These are the two oscilloscopes that are used to graphically represent the three different powers. The top oscilloscope is used to look at the reflected and transmitted powers while the bottom scope is used to look at the phase of the RF signal compared with the forward power.

To actually test a cavity, the resonant frequency is excited in the cavity using an RF signal generator. During a vertical cavity test, the cavity's resonant frequency cannot be changed except by external factors, such as temperature, so the RF input signal is adjusted to match that of the cavity under test. The RF signal frequency is recorded by the LabVIEW VIs. A LabVIEW VI is a virtual instrument that allows a user to connect and communicate with hardware and analyze data. This frequency is changing throughout the test as a result of the changing temperature and power. These VIs also record the forward, reflected and transmitted powers, the temperature and pressure of the helium bath and the decay time of the transmitted power. Using this data, the quality factor of the cavity and the accelerating gradient can be obtained.

In order to find the maximum accelerating gradient of the cavity, the helium pressure must be reduced to about 12 Torr. The reason for this is that at this pressure, a corresponding temperature of about 1.8K, liquid helium is below the superfluid lambda point of about 2.2K. Superfluid helium has better thermal conductivity which eases the process of keeping a cavity

cold. Additionally, superfluid helium has a property called second sound in which changes in temperature produce temperature or entropy waves. Using this property, quenches can be triangulated back to their origin.

During the pump down to 12 Torr, the accelerating gradient doesn't fluctuate much. This is done by keeping a constant peak transmitted power. The reason for this is that as the temperature decreases, the power dissipated decreases and the quality factor increases. Since the accelerating gradient is proportional to the square root of the product of the power dissipated and quality factor, the opposing directions of change approximately cancel out.

Once down at 12 Torr, the power is incrementally increased to find the maximum accelerating gradient. This is when a cavity is most likely to quench as the electromagnetic fields are approaching the critical fields at which superconductivity is lost and could excite electrons.

LabVIEW

Two different LabVIEW VIs are used to collect and analyze the test data. The reason for the two different VIs is that someone thought they could improve upon the initial VI. They wanted make the LabVIEW VI do analysis so there wasn't as much offline analysis to be done. Therefore, parts were added to specify the cavity type and set cable calibration constants.

With this improved upon VI, there was a known issue. This problem was it appeared the Z value for a 1.3 GHz Single Cell cavity was stuck in the VI (Figure 5). Equation 1 relates Z to various qualities of a cavity.

$$Z = \frac{\sqrt{\frac{R_{sh}}{Q_o}}}{L_{eff}} \quad (1)$$

In Equation 1, R_{sh} is the shunt impedance of the cavity, Q_o is the quality factor of the cavity and L_{eff} is the effective length of the cavity. The reason it appeared the Z value was stuck was that when $\frac{R_{sh}}{Q_o}$ or L_{eff} was changed, the Z value wouldn't recalculate.

The value of Z is used in calculating the accelerating gradient by Equation 2.

$$E_{acc} = Z\sqrt{Q_o P_{loss}} \quad (2)$$

Q_o is again the quality factor of the cavity and P_{loss} is the power lost in the cavity. Because Z was incorrect, the two different LabVIEW VIs gave different results for the accelerating gradient. Additionally, the two VIs gave different values for the quality factor. The reason for this will be

demonstrated later but has to do with the assumptions that are made involving the input coupling factor.

The compounding issue is the way in which the LabVIEW VI is written. It is written in a way that one wouldn't be testing a new cavity without restarting the VI. Therefore instead of having a column in the written spreadsheet including the values of $\frac{R_{sh}}{Q_o}$, L_{eff} and Z, these values are written in the header of the file. This means that once the spreadsheet has been made, the values are constant and to redo this would involve many changes to the VI.

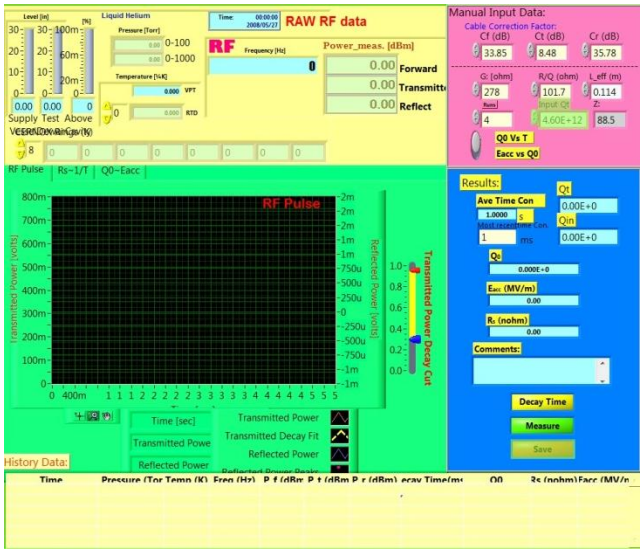

Figure 5 - This figure is of the LabVIEW VI in which the value of Z for a 1.3 GHz single cell cavity appears to be stuck. Even upon changing the values used to calculate Z, Z doesn't change.

Results and Discussion

Using the measurements obtained from the two different LabVIEW VIs, many things can be calculated. The first quantity that needs to be calculated is the loaded quality factor. This can be obtained using Equation 3.

$$Q_L = \frac{\omega \tau_{decay}}{2} \quad (3)$$

In Equation 1, Q_L is the loaded Q, ω is the angular excited frequency and τ_{decay} is the time it takes for the transmitted power to decay.

Once Q_L is known, the quality factor of the cavity, Q_o, can be obtained in a multitude of ways. The basic equation for finding Q_o involves using the input coupling, the transmitted power coupling and the loaded Q (Equation 4).

$$Q_o = (1 + \beta_{in})(1 + \beta_t)Q_L \text{ (4)}$$

β_{in} is the coupling factor at the input coupler while β_t is the coupling factor at the transmitted coupler where β_t is

$$\beta_t = \frac{P_t}{P_{loss}} \text{ (5)}$$

and P_t is the transmitted power and P_{loss} is the power lost. P_{loss} is calculated using Equation 6.

$$P_{loss} = P_f - P_r - P_t \text{ (6)}$$

In equation 6, P_f is the forward power and P_r is the reflected power.

For the first case, one assumes that the input coupler is tuned to unity and that the transmitted coupler is so small that is doesn't affect much. Therefore, the quality factor of the cavity is equal to two times the loaded Q. The second case also assumes that the input coupler is tuned to unity but that the value of the transmitted coupling factor does matter. This will increase the value found for Q_o.

The other two cases don't set the value of β_{in} to be one. However, in order to use these two analysis methods, one must know if the input coupler is over or under coupled. For the case of over coupling at the input coupler, the value of β_{in} is found by Equation 7.

$$\beta_{in} = \frac{1 + \sqrt{\frac{P_r}{P_f}}}{1 - \sqrt{\frac{P_r}{P_f}}} \text{ (7)}$$

In the above equation, P_r is the reflected power and P_f is the forward power.

In the case of under coupling at the input coupler, the value of β_{in} is the inverse of Equation 7. The reason for these sign conventions is that when you have the addition in the numerator, the value of the coupling coefficient is greater than one so the result is over coupling. Similarly, under coupling is when the value of the coupling coefficient is less than one and so subtraction occurs in the numerator.

After finding the quality factor of the cavity, the accelerating gradient can be obtained using Equation 2.

After finding the accelerating gradient, the transmitted power probe must be calibrated using the data. To do this, one must find the value of Q_t, the quality factor of the transmitted power probe. This can be done with a variation on the formula for Q (Equation 8).

$$Q = \frac{\omega U}{P} \quad (8)$$

The quality factor, Q, is the ratio of the energy gained, U, to the power lost, P, in one cycle, ω. ω is the angular frequency using the frequency currently being generated by the RF generator. By replacing P with P_t in Equation 8, one obtains the equation to find Q_t. U and ω are essentially constants especially when taken at a data point by data point basis. These two values are dependent on the cavity and not which power or quality factor one measures.

Q_t is then calibrated at an accelerating gradient of around five to eight megavolts per meter or at a medium accelerating gradient where the quality factor of the cavity is flat. This is done so that when there are other losses in power than to the cavity itself, they don't affect the calculation of the accelerating gradient. These losses could be power lost in the production of electrons.

After calibrating Q_t, one is able to again find the accelerating gradient by replacing Q_o and P_{loss} in Equation 2 with Q_t and P_t. Since the quality factor of the transmitted power probe is now held constant and the transmitted power is changing, we are able to obtain different accelerating gradients using a slight variation on Equation 2.

Once Q_t has been calibrated, one can multiply this by β_t to obtain Q_o. This again is based on the fact that for each point, no matter what Q one measures, U and ω are constant.

After data analysis, at least two graphs will be made. These two graphs are of the quality factor versus the temperature and the quality factor versus the accelerating gradient. The graph of the quality factor versus the temperature should appear to be a negative exponential indicating that as the temperature decreases, the quality factor increases. The quality factor increases because as the temperature is reduced, the surface resistance decreases as does the power dissipated. Since power dissipated is in the denominator of Equation 8, the smaller the power, the larger the quality factor.

The graph of the quality factor versus the accelerating gradient would ideally be a horizontally straight line until the cavity reaches its maximum accelerating gradient, at which time the quality factor would fall towards zero. For pure niobium, the theoretical maximum accelerating gradient is of order 60 MV/m. Due to impurities and current fabrication techniques,

good SRF cavities tend to max out around 30-35 MV/m with a handful of cavities worldwide achieving in excess of 40 MV/m. In reality, the quality factor is constant with increasing accelerating gradient but then starts to fall off gradually as power is dissipated to places other than the cavity itself. This can be due to imperfections and particulates inside the cavity, improper production procedures and impure niobium.

More information on the data analysis can be found in references one and four.

Table 1 – This is a table summarizing the following descriptions of the cavity tests performed.

Date	**Cavity ID**	**Cavity Type**	**Results**	**Comments**
06/07/11	F3A9	3.9 GHz 9-cell	Max Eacc = 23.1MV/m Max Q = 4.57E9	X-rays produced
06/30/11	F3A9	3.9 GHz 9-cell	Max Eacc = 26.5MV/m Max Q = 6E9	120°C bake prior to test Transmitted power meter head changed prior to test X-rays produced
07/19/11	T31F003	3.9 GHz 1-cell	Max Eacc = 19.2MV/m Max Q = 4.97E9	

F3A9

Cavity F3A9 is a 3.9 GHz 9 cell cavity fabricated at Fermilab. F3A9 had its inner surface treated using buffered chemical polishing (BCP). It was tested twice, once on June 7th and once on June 30th. The difference between the two dates is the cavity hadn't been baked at 120°C for a day or two before being tested on the 7th but had been baked before being tested on the 30th. Additionally, between testing on the 7th and testing again on the 30th, the transmitted power

meter probe was changed due to a nonlinear response discovered during analysis of previous test data and later verified empirically.

F3A9 June 07th, 2011

On June 7th, the temperature was 4.5K when data taking began with a corresponding pressure of 930 Torr. While pumping down to 12 Torr, data was taken to make a Q vs. T graph (Figure 6).

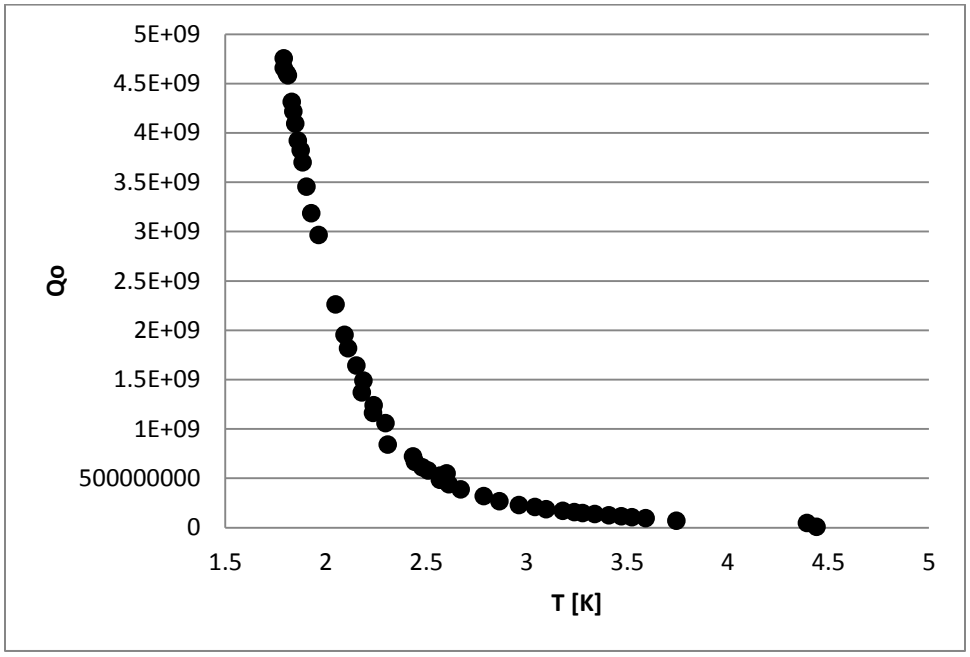

Figure 6 - Graph of the quality factor of the cavity versus the temperature of the liquid helium. This is a typical graph of this type. As the temperature decreases, the quality factor should increase like a negative exponential.

During pump down to 12 Torr, the cryosystem stalled and the pressure remained constant just above 30 Torr. More than two hours later, the cryosystem was able to recover and continue pumping down to 12 Torr. In order to pump down, the liquid helium in the dewar must cover the cavity but pumping must be done to reduce the pressure. As a result of pumping, the liquid level may drop, increasing the temperature of the cavity. Thus, a delicate balancing act between the liquid helium level and pressure is in play.

Once at 12 Torr, data was taken to find the maximum accelerating gradient of the cavity. During this time, the maximum accelerating gradient was found to be 23.1MV/m and the maximum quality factor was 4.57E9 (Figure 7). This was obtained using a Q_t of 5.81E10. The accelerating gradient was limited by a quench.

While taking data for the Q vs. Eacc graph, the pressure increased to around 25 Torr and the cryosystem had trouble pumping back down to 12 Torr. Therefore, there are two temperatures, 1.8K and 2K, in which the data points for the quality factor versus accelerating gradient graph were measured.

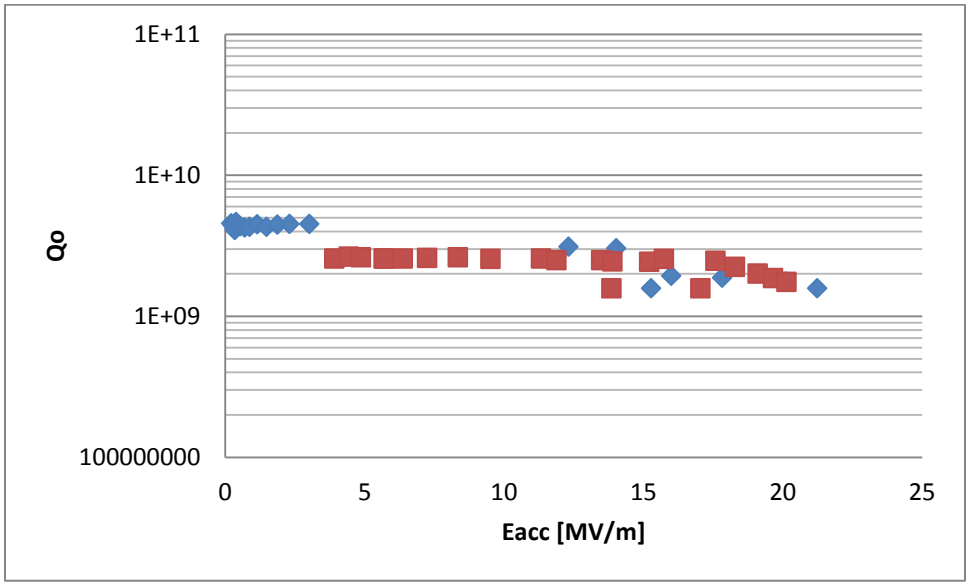

Figure 7 - Plot of the quality factor versus the accelerating gradient. The y-axis is a log plot of the quality factor. The appreciable drop in quality factor before 5MV/m is due to having taken data at 25 Torr due to issues with the cryosystem. The blue data points are from the 10-20 Torr data set and the red data points are from the 20-30 Torr data set.

The accelerating gradient was limited by a quench. Second sound and thermometry data were obtained for this quench. During testing, x-rays of up to 250 cpm were produced. This number is arbitrary. It is measured using a Geiger counter attached to the outside of the dewar. Other farther away calibrated devices for measuring dose are used that if enough radiation was detected would shut down testing. On this test, radiation was picked up by one of these calibrated counters. On all other tests, this didn't happen.

F3A9 June 30th, 2011

On June 30th, the first data point was taken at about 4.3K which corresponds to a pressure of about 830 Torr. The pump down to 12 Torr was relatively smooth. During this pump down, a smooth graph was obtained for the quality factor versus temperature (Figure 8).

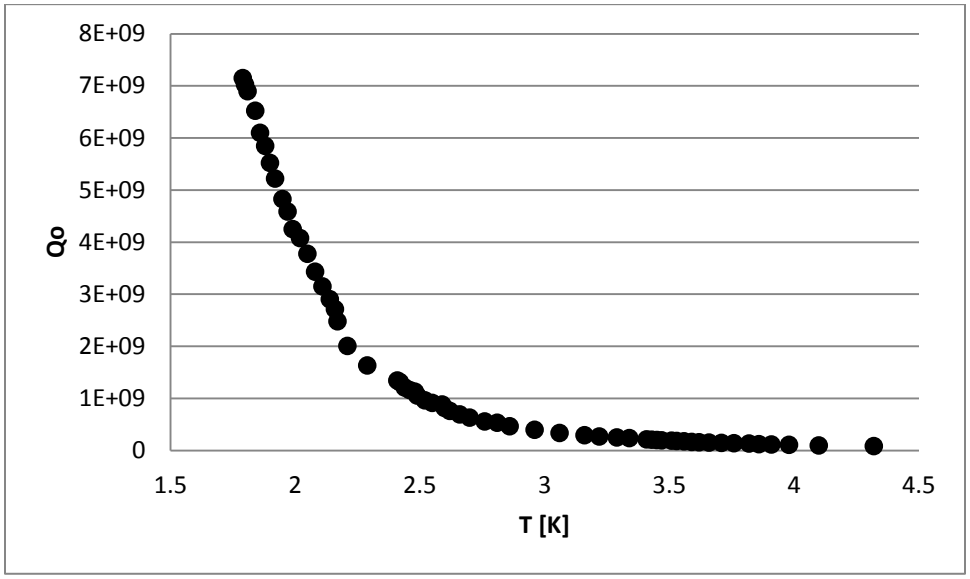

Figure 8 - Graph of the quality factor versus temperature from data obtained on June 30th.

During taking data for the Q vs E_{acc}, cryosystem instabilities again made maintaining a steady pressure of 12 Torr difficult. The pressure increased above 25 Torr and data was unable to be taken for an appreciable amount of time. Due to this, data was taken at 2K instead of the typical 1.8K. Eventually, the pressure was brought closer to 12 Torr.

The maximum quality factor for this test of F3A9 was 6E9. This cavity achieved a maximum accelerating gradient of 26.5MV/m. These numbers were obtained using a Q_t of 7.02E10. See Figure 9.

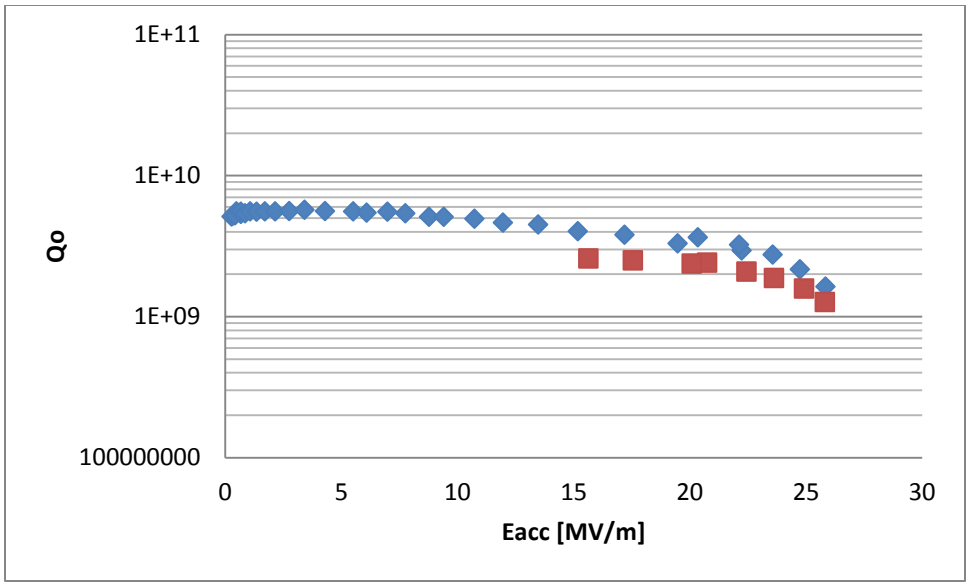

Figure 9 - The graph of the quality factor versus accelerating gradient. The plot appears to be relatively flat until about 10MV/m. The data set that is slightly lower than the others on the right half of the graph is the data that was taken around 25 Torr. The blue data points are from the 10-20 Torr data set and the red data points are from the 20-30 Torr data set.

The accelerating gradient was limited by a quench in which second sound data was available but no heating was evident. Additionally, x-rays were produced with up to 2000 cpm.

F3A9 Comparison

Comparing the data between the two tests, it appears that the cavity had a better test on the second day. By looking at the graphs of the quality factor versus temperature and the quality factor versus accelerating gradient, this is apparent as the curve for the second day is shifted up and to the right for each day (Figure 10). This means that a higher quality factor is obtained at higher temperature and would imply that the cavity performed better on the second day. Since the data is also shifted in the quality factor versus accelerating gradient graph, this implies that the cavity had a larger quality factor at the same accelerating gradients and that the cavity reached larger accelerating gradients (Figure 11).

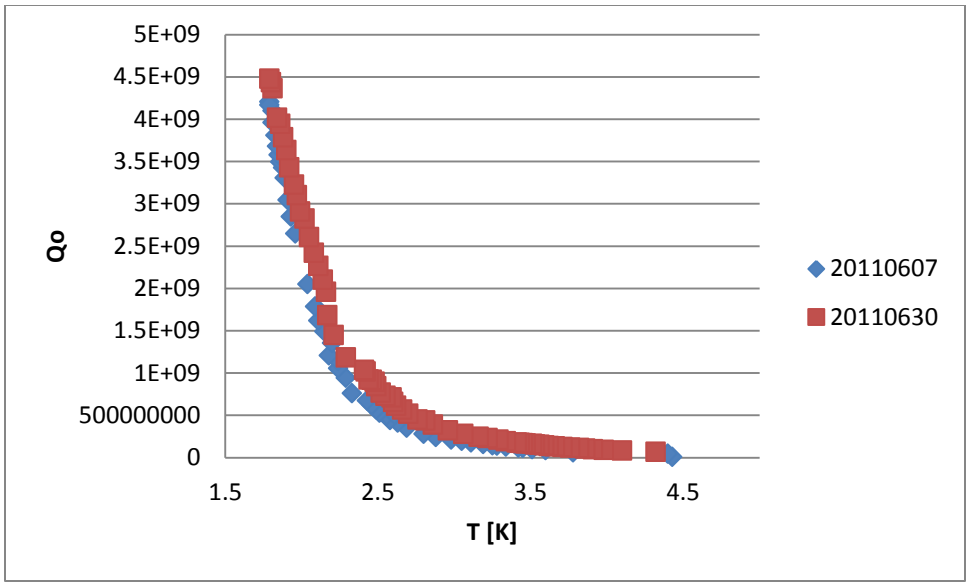

Figure 10 - The blue diamonds are the first data set taken on June 7th, 2011. The red squares are the second data set taken on June 30th, 2011. The second day appears to reach a higher quality factor at higher temperatures.

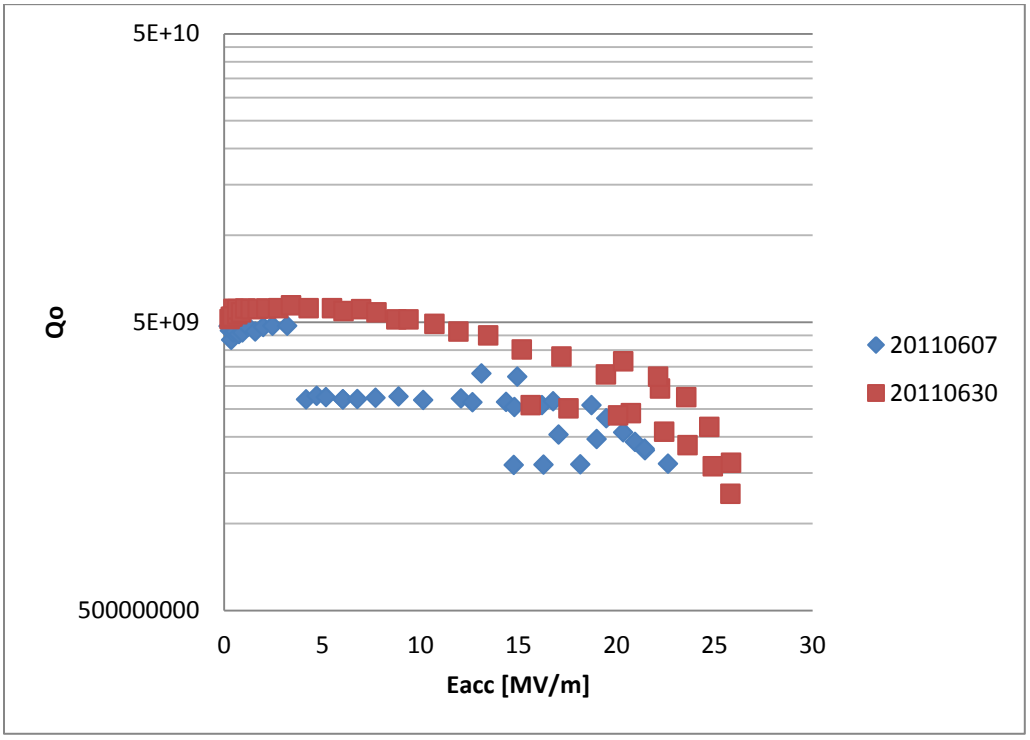

Figure 11 - The blue diamonds are data points from the first day of testing on June 7th, 2011. The red squares are data points from the second day of testing on June 30th, 2011. The second day appears to have performed better.

The difference between the two test dates is that the cavity was baked at 120°C for one to two days before being tested a second time. Additionally, the transmitted power meter probe was changed before the second test date. Baking a cavity is thought to increase the flat portion of a Q vs. Eacc graph. Due to this, is this seemingly better test due to being baked or the new transmitted power probe?

Since it doesn't appear to have elongated the flatness of the Q vs. Eacc curve, it appears this effect is due to the new transmitted power probe. The calibrated Q_t was much higher the second day which could be a result of a more linear transmitted power probe. However, since the data isn't taken at a consistent pressure on the first day, could it be that the since the pressure was higher and therefore the temperature was also higher, the quality factor was able to maintain one value for a longer period of time? Further testing must be done in order to see what, if any, effect baking the cavity had the quality factor versus accelerating gradient graph.

T31F003

On July 19th, 2011, cavity T31F003, a 3.9 GHz single cell cavity, was tested. This cavity was fabricated at Fermilab and like cavity F3A9, it had its surface treated using BCP. It is one of a series of single cell cavities being used for R&D evaluating various processing procedures. This is the only single cell cavity of the series to be BCP treated, all the others were EP treated. The first data point was taken around 4.3K with a corresponding pressure of about 830 Torr. The pump down to 12 Torr was quite uneventful. The quality factor versus temperature data obtain appeared to be as expected. (Figure 12) The quality factor increased as the temperature decreased.

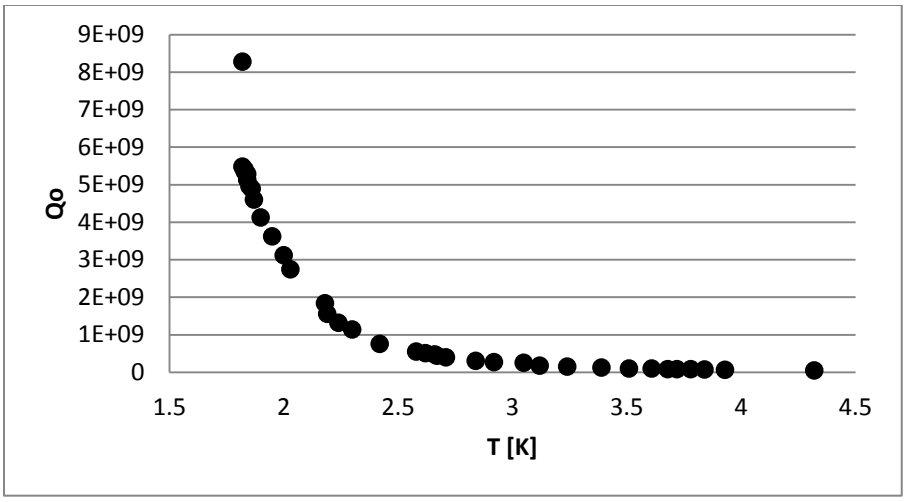

Figure 12 - Graph of the quality factor versus the temperature of T31F003. This graph appears to be as it should with two outliers.

The maximum accelerating gradient of this cavity was limited by a quench and found to be 19.2MV/m (Figure 13). The maximum quality factor was found to be 4.97E9. The quench was noticed on the oscilloscope that traces the reflected and transmitted power (Figure 14). Data was obtained about this quench in the form of second sound and thermometry.

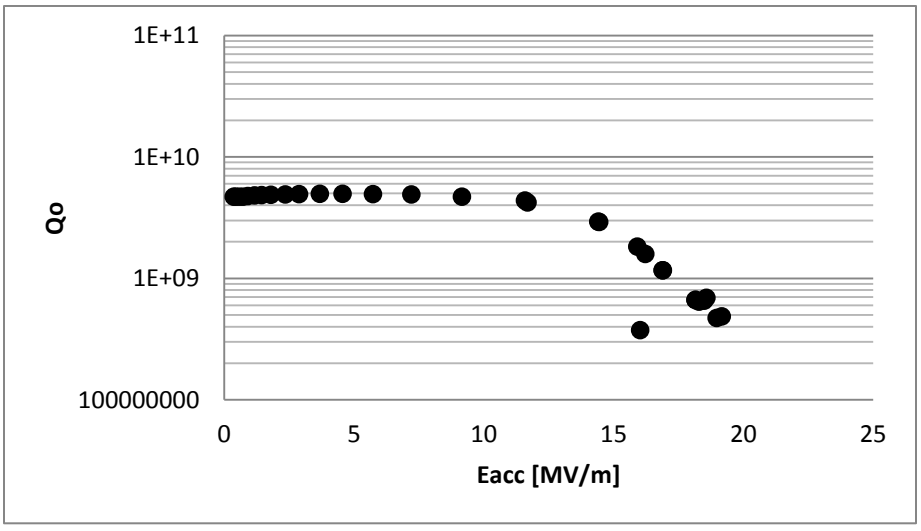

Figure 13 - Graph of the quality factor versus accelerating gradient. The quality factor appears to remain fairly flat as the accelerating gradient increases until about 11 or 12MV/m. No pressure issues occurred while obtaining this data so further inspecting may need to be done on the data point off trend after 15MV/m.

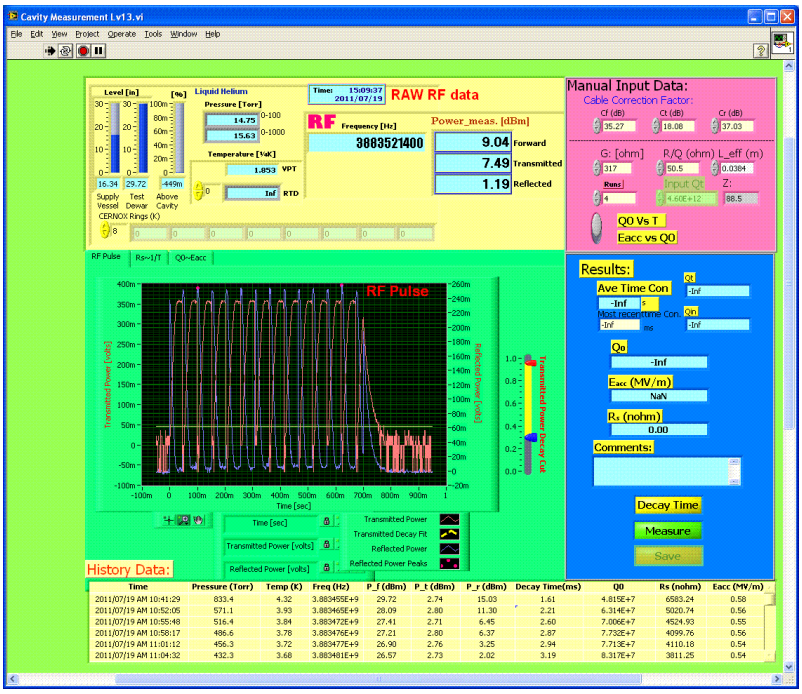

Figure 14 - This is the trace seen on the oscilloscope of the reflected and transmitted powers of the cavity during a quench. This is a typical signature as the reflected power will come to a maximum and then dissipate as the transmitted power goes to a maximum. It continues to happen as it takes the transmitted power a very short time to be dissipated.

LabVIEW

The problem with the LabVIEW VI again was that when either $\frac{R_{sh}}{Q_o}$ or L_{eff} where changed, the value of Z didn't recalculate. However, upon further investigation, it was discovered that the value of Z did recalculate if the values of $\frac{R_{sh}}{Q_o}$ or L_{eff} were changed before the run button was hit.

Due to habits while using this VI, something needed to be changed in order to have a more accurate depiction of the actual values while taking data. In order to remedy this, a prompt and a pull down menu were added (Figure 15). The prompt was to alert the user to select the type of cavity being tested. Four types of cavities are available to be chosen from the menu: 1.3 GHz Single Cell, 3.9 GHz Single Cell, 3.9 GHz 9 Cell and Other. If "Other" is selected, the user is prompted to input the necessary values for calculating Z and has ten seconds to comply.

When any of the other three options are selected, the values of $\frac{R_{sh}}{Q_o}$ and L_{eff} are updated and Z is calculated from these values. Now the values for the accelerating gradient output by the LabVIEW VI can be more trusted except in the regions previously talked about.

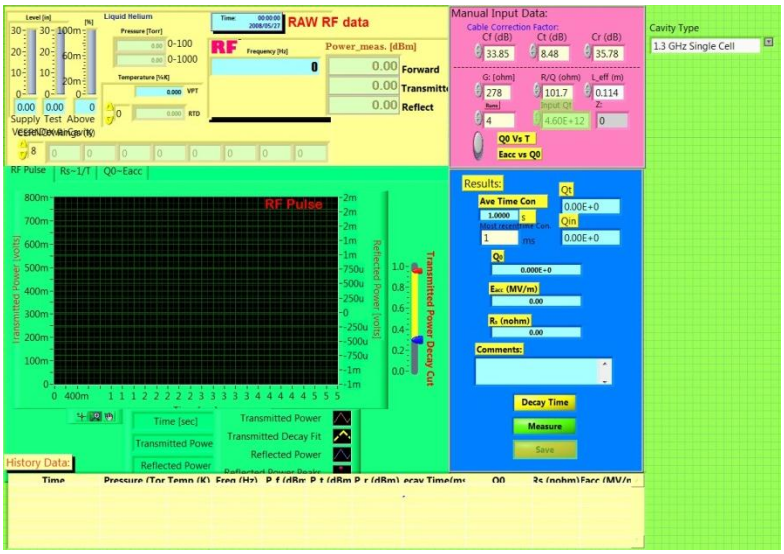

Figure 15 - Image of the new LabVIEW VI. The pull down menu is in the upper right corner of the VI. It allows you to select the cavity type or input the various cavity dependent qualities. This means experimenters can be more confident in the given output.

Conclusion

F3A9 was produced as a spare for a cryomodule for FLASH at DESY. According to design specifications, the accelerating gradient was to be 14 MV/m. Since the maximum accelerating gradient greatly exceeded this value, the cavity is going to be dressed encase a spare is needed.

T31F003 demonstrates why a single cell is tested before making production multi-cell cavities. Making a multi-cell cavity increases the complexity of fabrication and processing, thus increasing errors and difficulty of comparing processing techniques.

In general, testing a SRF cavity is a complex process. Thus, testing requires a well characterized system. A large component of this system is the power cables. Before each test, calibration of the power cables must be done. Incorrect calibration will give the wrong quality factor and accelerating gradient.

Another component of the testing system is the cryosystem. In all but one of the three cavity tests, cryosystem instabilities occurred. Due to this, the resulting graphs for the quality factor versus accelerating gradient were different from expected. The reason for this is that different pressures correspond to different temperatures. Since the pressure increased from the desired 12 Torr, the surface resistance of the cavity increased and the quality factor therefore decreased. Had the pressure remained constant, this graph might have appeared dramatically better.

Besides having cryosystem problems, changing the head on the transmitted power probe makes it difficult to show if baking a cavity had any effect on the Q vs. Eacc plot. The reason for this is that baking a cavity is thought to increase the flatness of the Q vs. Eacc curve. Since this curve was less flat the second time, it brings this into question. The other reason that the curve could have been shifted was that the new transmitted power probe is better calibrated than the old one was.

More testing must be done to decide if the shift in quality factor was due to baking or if it was due to having replaced the transmitted power probe. With the improved LabVIEW VI, testing cavities to see what effect baking or the new transmitted power probe have should be expedited. This reason being that the improved VI should reduce the amount of offline analysis needed thus expediting the results of cavity tests.

Post Script

After I had completed my internship at Fermilab, another cavity test was run on T31F004. Before running this test, it was discovered that pieces of foam insulation at the top of the dewar had shrunk appreciably. New insulation was installed. The test had a very smooth pump down to 12 Torr. Additionally, Q vs. Eacc data was able to be taken at three different temperatures with constant pressures throughout each temperature set, especially at 1.6 and 1.8K. This is something that was recently impossible. Though this has only been tested once, it appears to have fixed the cryosystem stability issues and we remain hopeful that future tests are as successful!

Acknowledgements

Thank you to Elvin Harms for being my mentor, Dr. Helen Edwards for helping to answer my questions, Dr. Hasan Padamsee for sharing his wealth of knowledge with me and

others in the form of his two books, RF Superconductivity for Accelerators and RF Superconductivity, Dr. Denis Kostin from DESY for his insightful views on quenches and SRF testing in general, Dr. Eric Prebys for allowing me to be part of this internship, Carol Angarola for coordinating this internship, my fellow A0 Portacamps workers, the other scientists and people I came into contact with at Fermilab, and my fellow interns at Fermilab (especially my fellow Lee Teng Interns at Fermilab and Argonne).

References

[1] Edwards, Helen. *3.9 GHz 9c9 Cavity Vertical Tests*. Notes. Print.

[2] Padamsee, Hasan, Jens Knobloch, and Tom Hays. *RF Superconductivity for Accelerators*. Weinheim: Wiley-VCH, 2008. Print.

[3] Padamsee, Hasan S. *Rf Superconductivity: Science, Technology and Applications.* Weinheim: John Wiley & Sons, 2009. Print.

[4] Saito, K. "6. Performance Evaluation." Lecture.

Appendix A